Effect of Welding Parameters on the Weld Bead Geometry of Low Alloy Steel using FCAW – Empirical Modeling Approach

A. Almazrouee, T. Shehata and S. Oraby

***Abstract*—**Quality of the weld bead is always governed by its geometry and configuration which, in turn are controlled by various welding process input parameters such as welding speeds, current, and voltage as well as the type of the welding process. Flux cored arc welding process is known to provide good control over heat input through the utilization of the process variables that can ensure an advance determination of the optimal bead geometry. The objective of the current investigation is to relate the geometry elements of the flux cored arc welding bead; height, depth of penetration and bead width to the welding operating parameters; traverse speed, voltage and amperage. This is carried out considering various types of shielding gases. For each segment of the above mentioned bead geometry-operating parameters relationship, experimental data are used to develop the relevant best mathematical model using linear and nonlinear regression techniques. Developed models are examined against their adequacy and significance and, are further validated using additional verification experimental data. Generally, the employed voltage and the weld speed tend to affect, to different extents, each of the bead geometrical elements with negligible effect of the amperage. Type of the shielding gas tends to have a predominant effect especially on the on the weld bead width.

***Keywords*—**Bead geometry, welding parameters, FCAW, shielding gas, regression modeling

I. Introduction

WELDbead geometry is usually controlled by various welding process input parameters such as welding speed, current, voltage, arc efficiency, preheating temperature, thermal conductivity, thermal diffusivity, and plate thickness [1]. As the liquid weld metal solidifies, the resulting interfacial tensions usually determine the final bead geometry [2]. The bead cross-section area usually determines the total shrinkage and consequently the internal residual stress and distortion [3]. Weld bead geometry also has a significant influence in the determination of the mechanical properties of the welded structure [4].

Many studies were performed to develop mathematical models that correlate the input parameters with the bead geometry dimensions. For example, mathematical models

were established to predict the geometry of the weld bead in the deposition of 316L stainless steel onto structural steel IS 2062 using GMAW [5]. The effects of current, electrode polarity, electrode diameter and, electrode extension on each of the melting rate, bead height, bead width and weld penetration were also studied [6]. Nagesh and Datta[7] studied TIG welding process and used multiple linear regression technique to develop mathematical models for weld bead shape parameters, considering the effects of main variables as well as their two factor interactions. However, only limited studies focused on the FCAW process. The effect of the input process parameters on duplex stainless steel clad quality parameters to accelerate the desired clad qualitywas studied [8]. Identification ofthe most influential process parameters on the bead geometry and the investegatation of the parameters that must be most carefully controlled were performed[9]. The study also showed that main interaction effects of the process variables played a major role in the detemination of the bead dimensions [10].

It is intended in the current study to investigate the response of low alloy steel toward welding parameters of FCAW process and to find correlation between the main parameters of heat inputs; welding voltage (V); welding current (A); and welding traverse speed (TS) and the bead geometry dimensions; width (W), height (H), and depth of penetration (P). These are investigated considering various types of shielding gases. Practical efficient mathematical models are postulated, developed using experimental results, and finally examined for their adequacy, significance, and empirical validation. Once approved and validated, the resulting model is considered liable for the in advance prediction of the weld bead geometry dimensions as influenced by heat input operating parameters within the design stage.

II. Experimental Work

Bead-on-plate method was employed using a low alloy steel plate with a chemical composition given in Table I and dimensions in Fig. 1a. Three types of shielding gases were used: Argon (A); CO_2(C); mixed gas77% Argon, 23% CO_2 (M). The plate was then left to cool down to room temperature without insulation. For investigation, a 10 mm width coupon was cut 50 mm away from the periphery of the plate, as shown in Fig. 1b. For each experiment, three runs were taken under the same conditions of voltage, traverse speed, and shielding gas.

The wire diameter used in this study was 1.2 mm, whereas the wire feed rate for all groups was constant at 3600 mm/min.

A. Almazrouee is with the College of Technological Studies, PAAET, Kuwait, (e-mail: aalmazro1@gmail.com).

T. Shehata is with Civil Engineering Department, Monash University, Victoria, Australia (e-mail: tarek_shehata@yahoo.com).

S. Oraby is with the College of Technological Studies, PAAET, Kuwait, (corresponding author, phone: +965 99549019; fax: +965 24832761 e-mail: samyoraby@hotmail.com).

The tip to work distance was 22 mm and an extension wire distance of 10 mm was kept fixed throughout the experiments. Each group contained four welding traverse speeds, (360, 420, 480 and 540 mm/min). The welding voltages were changed with each speed to four different levels (23, 25, 28 and 32 volts).This led to a factorial experimental design of 16 tests for each shielding gas. For each experiment the weld bead geometry parameters W, H, and P (Fig. 1c) were measured. These dimensions were measured for the three runs, having the same conditions, and then the three readings were recorded, and then averaged. The measurements of bead geometry elements were taken from polished and etched transverse cross sections of each weld. Measurements of bead dimensions were carried out using a binocular microscope equipped with a calibrated reticule. Table II lists the entire set of the experimental work performed. Each experimental data set included 16 cases of which 12 cases were used to estimate the models coefficients while the other 4 cases were used to validate the developed final model; cases 3, 7, 9, and 16, Table II. Such validation experiments were selected to cover the entire operating domain and their boundaries. This has led to the development of the different functional interrelationships as indicated through the following sections.

TABLE II
NOMINAL CHEMICAL COMPOSITION OF THE STEEL PLATE

No	Elements	%
1	Fe	Bal.
2	C	0.12
3	Si	0.13
4	Mn	0.63
5	P	0.02
6	S	0.01
7	Ni	0.02
8	Cr	0.01
9	Mo	<0.01
10	Cu	<0.01
11	V	<0.01
12	Ti	<0.01
13	Co	<0.01
14	Al	<0.03

III. MATHEMATICAL MODELING PROCEDURES

Both multiple linear and nonlinear regression routines are used to fit the available experimental measurements into the model. A first order linear model is proposed to relate response (R) to the parameters in their natural values (ξ J) taking the form:

$$R = bo + \sum_{j=1}^{p} b_j \xi_j + \varepsilon_n , \quad (1)$$

where$\epsilon_n$is the error absolute value using linear non-transformed model while b_0 and b_j are the estimated values of the model coefficients.

Although the model (1) can be fitted satisfactorily to many combinations of operations parameters, there is still a number of experimental situations where a model of the type described is not satisfactory because the data clearly shows the existence of nonlinearities which cannot be ignored. Therefore, it is necessary to introduce models which take care of possible non-linearity and interaction which might exist among the operating parameters. Therefore, Second-order model structure is introduced to take the general form:

$$R = b_o + \sum_{j=1}^{p} b_j \xi_j + \sum_{j=1}^{p} \sum_{k \geq j}^{p} b_{jk} \xi_k + \varepsilon_n \quad (2)$$

For sake of comparison with linear regression model form (1), the general multiplicative nonlinear regression model to relate a measured response (R) for (P) independent variables is proposed:

$$R_F = c \prod_{j=1}^{p} \xi_j^{\beta j} \varepsilon^{\wedge}, \quad (3)$$

in which $\varepsilon^{\wedge}$ is the multiplicative random error.

Many statistical criteria are used to examine the significance and the adequacy of the resulting models. These are the Correlation factor R^2, the F-ratio and t-statistic value.

IV. RESULTS AND DISCUSSION

A. Effects of welding controlling parameters on bead height (H

According to Table III, the resulting significant and adequate linear and nonlinear models for bead height for Gas A, HA, are:

$$H_{A=} 4.572 - 0.003\ (TS) - 0.039\ (V) \quad (4)$$

$$H_A = 407.19\ (TS)^{(-0.604)} (V)^{(-0.481)} \quad (5)$$

The amperage (A) was not significant enough to enter the final equation. The effects of both TS, as a primary controlling variable, and V are evident where they are found to have, to different extents, a negative influence on the H, Fig. 2. For a given value of V, H tends to decrease as TS is increased and, the same trend is observed regarding the effect of increasing voltage at constant TS. Developed models for Gas C and Gas M are:

$$H_C = 6.165 - 0.004\ (TS) - 0.078\ (V) \quad (6)$$

$$H_C = 142283\ (TS)^{(-0.58)} (V)^{(-0.861)} \quad (7)$$

$$H_M = 4.894 - 0.004\ (TS) - 0.037\ (V) \quad (8)$$

$$M_M = 662013\ (TS)^{(-0.715)} (V)^{(-0.406)} \quad (9)$$

As shown by Fig. 3-5, models validation is examined by comparison the output (H) from both models to those experimentally obtained by the validation four cases, Table II. Again, the nonlinear model indicates a slight superior predictability over the linear form. For gas C, either linear or nonlinear estimates correlate very well with the verification experimental cases. However, for case #16 where maximum values of all operating parameters are employed, both models underestimate the output with better predictability of the nonlinear form, Fig. 4. In contrast, when low TS is employed at low V using Gas M, case #3, Fig. 5, both models seem to overestimate the experimental measured values.

B. Effects of welding controlling parameters on penetration depth (P)

Regarding the relationship between the bead depth (P) and the operating parameters; TS, V, and A, modeling procedures led to the most adequate significant models 10-12 with only the significant parameter(s) are included.

$$P_A = 0.005.(Amp),$$
$$(R^2 = 92.2,\ SE = 0.156,\ F = 13,\ t_{\beta 3} = 12) \quad (10)$$

$$P_C = 0.49 + 0.066.(V),$$
$$(R^2 = 61.9,\ SE = 0.19,\ F = 16.3,\ t_{\beta 0} = 1.11,\ t_{\beta 2} = 4.03) \quad (11)$$

$$P_M = 168.025.(TS)^{-0.783},$$
$$(R^2 = 60.8,\ SE = 0.148,\ F = 566,\ t_{\beta 1} = -4.0) \quad (12)$$

This indicates that the bead depth (P) is basically affected by the amperage (A), the voltage (V), and the traverse speed (TS) for Argon, CO_2, and mixed gas respectively. Validation procedures are shown in Figure 6 with good correlation.

C. Effects of welding controlling parameters on the bead width (W)

As indicated by models 10-12 for all gases, the weld bead width (W) is found to be positively affected by (V) while it is negatively affected by the traverse speed (TS) at less impact. Validation analysis is illustrated in Fig. 6.b.

TABLE II
EXPERIMENTAL OPERATING PARAMETERS AND MEASURED WELD BEAD GEOMETRY

Test Seq.	TS	V	Gas A (Argon)				Gas C (CO_2)				Gas M (Mixed)			
			Amp	H	P	W	Amp	H	P	W	Amp	H	P	W
a) Experimental data for models estimation														
1	360	23	180	2.5	0.983	7.573	225	3.097	2.075	9.405	160	2.5	0.895	7.235
2	360	25	190	2.425	1.01	8.337	215	2.898	2.25	9.325	170	2.455	1.088	8.635
4	360	32	200	2.232	1.483	9.268	230	2.29	2.475	13.535	160	2.318	1.607	9.495
5	420	23	160	2.403	0.925	6.97	210	3.048	1.94	8.29	170	2.318	1.003	7.74
6	420	25	170	2.315	1.113	8.163	215	2.69	2.165	8.39	173	2.182	0.823	7.775
7	420	28	190	2.148	1.078	8.375	220	2.367	2.372	10.37	175	2.102	0.627	8.92
8	420	32	200	2.114	0.758	8.855	225	2.21	2.322	11.97	176	2.032	0.533	7.78
10	480	25	175	2.04	1.173	6.798	225	2.488	2.183	8.58	175	1.972	0.638	6.645
11	480	28	160	1.985	1.021	6.913	230	2.31	2.417	9.585	170	1.86	0.452	6.89
12	480	32	170	1.827	0.318	6.238	235	2.124	2.867	10.185	160	1.652	0.33	6.395
13	540	23	160	2.153	0.642	5.155	220	2.505	1.868	5.635	160	1.852	0.633	5.505
14	540	25	160	1.965	0.917	5.975	225	2.197	1.924	6.955	150	1.65	0.567	6.2
15	540	28	150	1.605	0.75	6.627	230	2.06	2.61	8.255	170	1.595	0.297	6.58
b) Verification experimental data for models validation														
3	360	28	190	2.372	1.107	8.648	220	2.72	2.302	11.625	180	2.39	1.305	9.26
7	420	28	190	2.148	1.078	8.375	220	2.367	2.372	10.37	175	2.102	0.627	8.92
9	480	23	170	2.215	0.717	6.367	220	2.693	1.932	7.04	180	2.127	0.85	7.475
6	540	32	150	1.538	0.328	5.455	238	2.017	3.152	8.45	175	1.465	0.223	6.555

TABLE III
SUMMARY OF MODELING RESULTS AND STATISTICAL CRITERIA FOR (H)ETRY

Gas Type	Linear Model: $H = \beta_o + \beta_1 (TS) + \beta_2 (V)$						Nonlinear Model: $H = \beta_o (TS)^{\beta_1} (V)^{\beta_2}$					
	($t\ \beta_o$)	($t\ \beta_1$)	($t\ \beta_2$)	R^2	SE	F	($t\ \beta_o$)	($t\ \beta_1$)	($t\ \beta_2$)	R^2	SE	F
A	15	-7.4	-4.7	88.7	.098	35	1.46	-6.4	-4.1	86.6	.105	1670
C	19.7	-8.3	-9.2	93.9	.099	69	1.88	-8.06	-9.2	94.2	.095	2812
M	29.9	-16.3	-8.2	97.2	.053	158	3.07	-15.9	-7.4	97.1	.055	6817

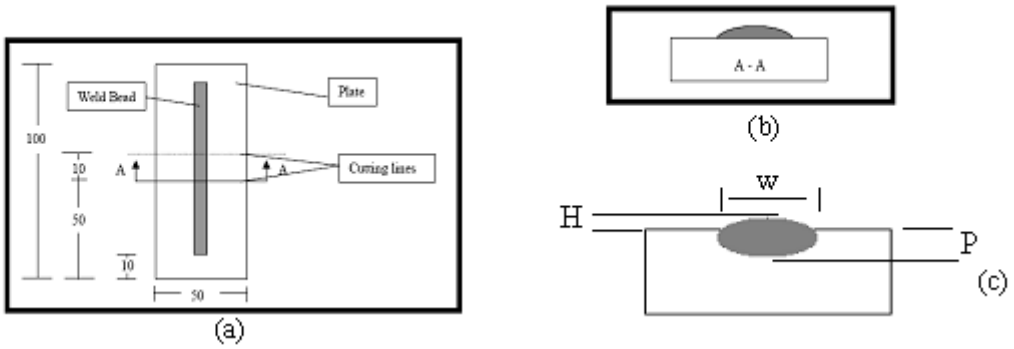

Fig. 1Schematic illustration of a) bead-on-plate welding and the cutting lines of the studied specimen b) the studied specimen cross-section A-A and c) weld bead geometry elements

$$W_A = 269.86\,(TS)^{(-0.861)}\,(V)^{(0.466)},$$
$$(R^2 = 81.6,\ SE = 0.582,\ F = 631,\ t_{\beta 0} = 0.9,\ t_{\beta 1} = 5.6,\ t_{\beta 2} = 9.5) \quad (13)$$

$$W_C = 23.756\,(TS)^{(-0.814)}\,(V)^{(1.218)},$$
$$(R^2 = 94.3,\ SE = 0.552,\ F = 1154,\ t_{\beta 0} = 1.15,\ t_{\beta 1} = 6.96,\ t_{\beta 2} = 9.44) \quad (14)$$

$$W_M = 59.03\,(TS)^{(-0.543)}\,(V)^{(0.423)},$$
$$(R^2 = 68.2,\ SE = 0.688,\ F = 301,\ t_{\beta 0} = 0.895,\ t_{\beta 1} = 3.57,\ t_{\beta 2} = 8.63) \quad (15)$$

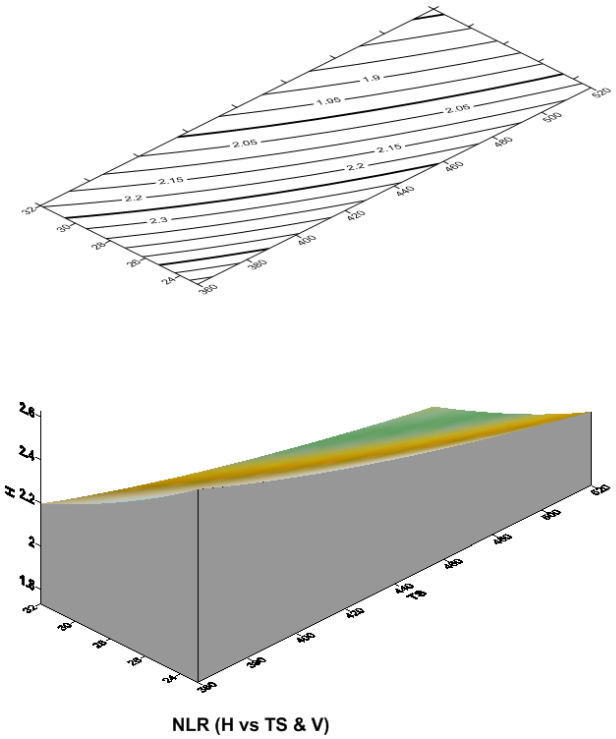

Fig. 2 Response Surface and Contour plots for H-TS-V relationship

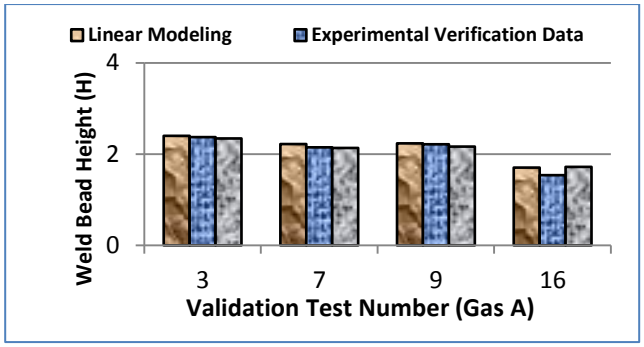

Fig. 3 Data Validation for Gas A (argon)

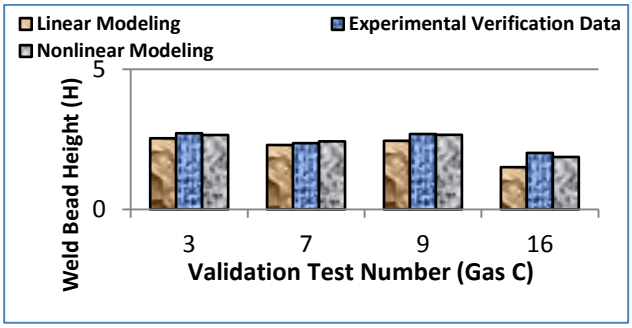

Fig. 4 Data Validation for Gas C (CO_2)

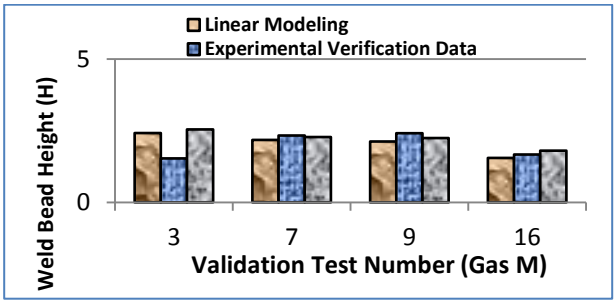

Fig. 5 Data Validation for Gas M

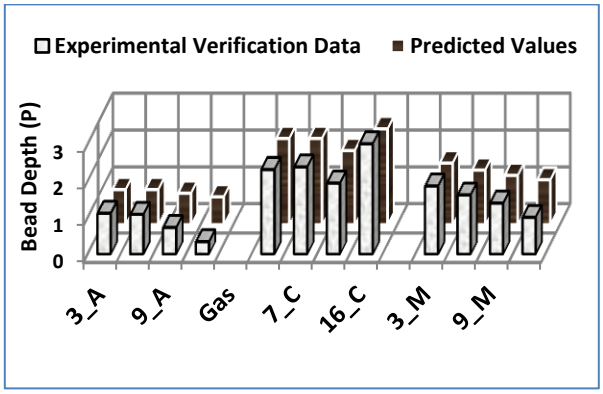

a) Bead Depth

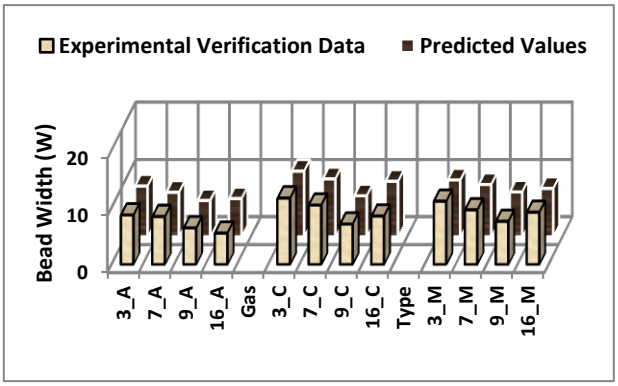

b) Bead Width

Fig. 6 Validation procedures for the weld bead depth at different shielding gases

V. CONCLUSIONS

The effects of the main welding process inputs on weld bead geometry variables when bead-on-plate welds are deposited using FCAW process have been investigated, modeled, and validated. Functional conclusions and concluding remarks can be summarized as:

Weld bead height (H) is negatively affected by the employed voltage (V) to greater extent than the traverse speed (TS). The amperage (Amp) is found to have an insignificant influence on (H). It is observed that that the voltage (V) has its greatest effect when CO_2 is employed as a shielding gas.

For Gas A, the amperage (Amp) is found to be the only parameter affecting (P) while individual effect of the voltage (V) and the traverse speed (TS) is observed for gases C and M respectively.

As far as the weld bead width (W) is concerned, both the voltage (V) and the traverse speed (TS) provide a contradictory influence. While increasing (V) increases width (W), an increase in (TS) tends to lead to less bead width. Employed voltage (V) tends to have its strongest influence on (W) when Gas C is employed while traverse speed (TS) indicates its lowest effect at Gas M.

REFERENCES

[1] A. S. Azar S. K. Ås, et al., "Determination of welding heat source parameters from actual bead shape," *Computational Materials Science*, vol. 54, pp. 176-182, 2012.

[2] K. Ishizaki, "Interfacial tension theory of the phenomenon of arc welding-mechanism of penetration," *Proceeding of Symposium on Physics of Arc Welding*, The institute of welding, London, pp. 195 – 209, 1962.

[3] A. Shumovsky, "Controlling welding shrinkage and distortion," *The Canadian Welder*, pp. 179 – 180, 1952.

[4] V. Dey, D. K. Pratihar, et al., "Optimization of bead geometry in electron beam welding using a Genetic Algorithm," *Journal of Materials Processing Technology*, vol. 209, no. 3, pp. 1151-1157, 2009.

[5] N. Muruganand R. S. Parmar, "Effects of MIG process parameters on the geometry of the bead in the automatic surfacing of stainless steel," *Journal of Materials Processing Technology*, vol. 41, no. 4, pp. 381-398, 1994.

[6] R. S. Chandel, H. P. Seow, et al., "Effect of increasing deposition rate on the bead geometry of submerged arc welds," *Journal of Materials Processing Technology*, vol. 72, no. 1, pp. 124-128, 1997.

[7] D. S. Nageshand G. L. Datta, "Genetic algorithm for optimization of welding variables for height to width ratio and application of ANN for prediction of bead geometry for TIG welding process," *Applied Soft Computing*, vol. 10, no. 3, pp. 897-907, 2010.

[8] T Kannan, and N. Murugan, "Effect of flux cored arc welding process parameters on duplex stainless steel clad quality," *Journal of Materials Processing Technology*, vol. 176, nos. 1-3, pp. 230-239, 2006.

[9] P. K. Palani. and N. Murugan, "Sensitivity Analysis for Process Parameters in Cladding of Stainless Steel by Flux Cored Arc Welding," *Journal of Manufacturing Processes*, vol. 8, no. 2, pp. 90-100, 2006.

[10] P. K. Palaniand N. Murugan, "Optimization of weld bead geometry for stainless steel claddings deposited by FCAW," *Journal of Materials Processing Technology*, vol. 190, nos. 1-3, pp. 291-299, 2007.